Observational Study

Medicine®

OPEN

Testicular tumors: discriminative value of conventional MRI and diffusion weighted imaging

Weiwei Wang, MD, Zhanguo Sun, PhD, Yueqin Chen, MD, Fan Zhao, MD, Hao Yu, PhD, Xiang Guo, MD, Kewei Shi, MD*

Abstract

To explore the feasibility of using conventional MRI features combined with apparent diffusion coefficient (ADC) values for the differential diagnosis of testicular tumors.

A total of 63 patients with pathologically confirmed testicular tumors were enrolled in this study. In particular, there were 46 cases of malignant lesions and 17 cases of benign lesions. All patients underwent conventional magnetic resonance imaging (MRI) and diffusion weighted imaging. Multivariate logistic regression models and receiver operating characteristic curves were constructed to assess diagnostic accuracies.

T2-homogeneity, intratumoral septa, and peritumoral infiltration were more common in the malignant group, and capsule sign was more common in the benign group ($P < .05$ for all). The mean ADC value of the malignant group was lower than that of the benign group ($P < .05$). When the ADC value $\leq 0.90 \times 10^{-3}$ mm^2/s, the diagnosis tended to be malignancy. The conventional MRI model could achieve better diagnostic accuracy than ADC values alone ($P < .05$). Compared with the conventional MRI model, the specificity and accuracy of the full model (ADC and conventional MRI model) increased by 9.8% and 3.2%, respectively. T2-homogeneity and T2-hypointensity were more common in seminoma and lymphoma, cystic changes were more common in nonseminomatous germ cell tumor (NSGCT), and intratumoral septa was more common in seminoma ($P < .05$ for all). The ADC value of NSGCT was larger than seminoma, and lymphoma was the smallest ($P < .05$ for all). Cystic changes, T2-hypointensity, intratumoral septa, and ADC value were independent factors for differentiating the seminoma, NSGCT, and lymphoma subgroups.

A combination of conventional MRI features and ADC values can improve the diagnostic efficiency for differentiating benign and malignant testicular tumors, and can additionally distinguish different subtypes of malignant testicular tumors.

Abbreviations: ADC = apparent diffusion coefficient, AUC = area under the ROC curve, DWI = diffusion weighted imaging, ICC = intra-class correlation coefficient, MRI = magnetic resonance imaging, NSGCT = nonseminomatous germ cell tumor, ROC = receiver operating characteristic, ROIs = regions of interests.

Keywords: apparent diffusion coefficient, diffusion weighted imaging, magnetic resonance imaging, testicular tumor

1. Introduction

Testicular tumors are rare in the general population, representing just 1% to 1.5% of all male tumors, but the majority (95%) are malignant.[1] Benign testicular tumors are generally treated conservatively to preserve normal testicular function, while malignant tumors are treated by radical resection and chemo-radiotherapy.[2,3] Seminomas are extremely sensitive to chemo-radiotherapy with generally good prognoses. In contrast, radiotherapy is not typically used for the treatment of non-seminomas and lymphomas on account of clinical aggressiveness.

Although needle biopsy is the gold standard for confirming the diagnosis of tumor, it is an invasive procedure and cannot be used to determine the range of the lesion. Computed tomography exposes the human body to radiation, and therefore the preoperative qualitative value for the tumor is limited.[4] Magnetic resonance imaging (MRI) is a powerful alternative modality for the evaluation of testicular masses and is mainly recommended in cases of nondiagnostic or equivocal sonographic findings.[5] However, the conventional MRI features of different subtypes of testicular tumors are overlapping and radiologists always estimate these imaging features in a subjective manner. Diffusion-weighted imaging (DWI) can quantify the diffusional mobility of water protons in biological tissues with apparent diffusion coefficient (ADC).[6–8] Thus, DWI provides functional information that can complement the structural or anatomic information obtained from conventional MR imaging. Another advantage of DWI is that it does not require intravenous contrast media, thus enabling its use in patients with renal dysfunction.[9] Previous studies have demonstrated the potential value of DWI or conventional MRI alone in the diagnosis of testicular tumors.[10,11] However, few studies have systematically

Editor: Gaurav Sharma.

The authors have no funding and conflicts of interest to disclose.

The datasets generated during and/or analyzed during the current study are available from the corresponding author on reasonable request.

Department of Medical Imaging, The Affiliated Hospital of Jining Medical University, Jining, China.

* Correspondence: Kewei Shi, No. 89 Gu Huai Road, Jining 272029, China (e-mail: shikewei0806@sina.com).

How to cite this article: Wang W, Sun Z, Chen Y, Zhao F, Yu H, Guo X, Shi K. Testicular tumors: discriminative value of conventional MRI and diffusion weighted imaging. Medicine 2021;100:48(e27799).

Received: 24 November 2020 / Received in final form: 16 September 2021 / Accepted: 28 October 2021

http://dx.doi.org/10.1097/MD.0000000000027799

elucidated the combined usage of DWI and conventional MRI features for the differential diagnosis of testicular tumors. To address these limitations, the purpose of this study was to assess the benefit of adding DWI to conventional MRI protocols for the differential diagnosis of testicular lesions.

2. Methods

2.1. Patients

From January 2013 to October 2019, 97 patients with testicular tumors were recruited and underwent conventional MRI and DWI, which were subsequently analyzed. The patient screening process and the exclusion criteria are demonstrated in the flow chart in Fig. 1. In total, 63 patients (average age: 40 ± 16 years; range: 22–71 years) with testicular tumors confirmed by pathology were enrolled in the current study, 46 were malignant tumors and 17 were benign lesions. Fifty-three cases complained of painless masses with progressive swelling, and the other 10 cases presented with scrotal tenderness. This study was approved by the institutional review board of our university and the need to obtain informed consent was waived. The decision number was 2020C031.

2.2. Image acquisition

MR examinations were performed on 3.0 T MR scanners (MAGNETOM Verio, Siemens, Erlangen, Germany) using an 8-element phased array matrix coil for signal reception. The patients were positioned in a feet-first supine position with the testes placed at a similar distance from the coil, by placing a towel beneath them, and with the penis draped on the lower anterior abdominal wall. The sequences utilized for each patient included axial fat-suppressed T1-weighted sequence (TR/700 ms; TE/13 ms) and fat-suppressed T2-weighted sequence (TR/4000~6000 ms; TE/80~100 ms). Moreover, DWI was acquired before contrast injection using single-shot spin-echo echo-planar imaging. The parameters were as follows: TR/TE = 5000/80 ms, signal averages = 3, and b values of 50 and 1000 s/mm^2. Axial and coronal gadolinium contrast-enhanced T1-weighted images were also obtained after the administration of a contrast agent (gadolinium diethylene triamine pentaacetic acid; 0.2 mL/kg body weight; Magnevist; Bayer Schering, Guangzhou, China). The field of view for all scans was 260 × 260 mm^2, the matrix size 384 × 320, the slice thickness 5 mm, and the interslice gap 0.5 mm.

2.3. Image analysis

Two radiologists (SK and WW) with 15 and 5 years of experience in pelvic MRI, blinded to the clinical details and pathology results, reviewed the MR images. The following conventional MRI features of the testicular tumors were evaluated: T2-hypointensity (lower signal intensity compared to the normal testicle parenchyma); cystic changes (areas of hyperintensity on

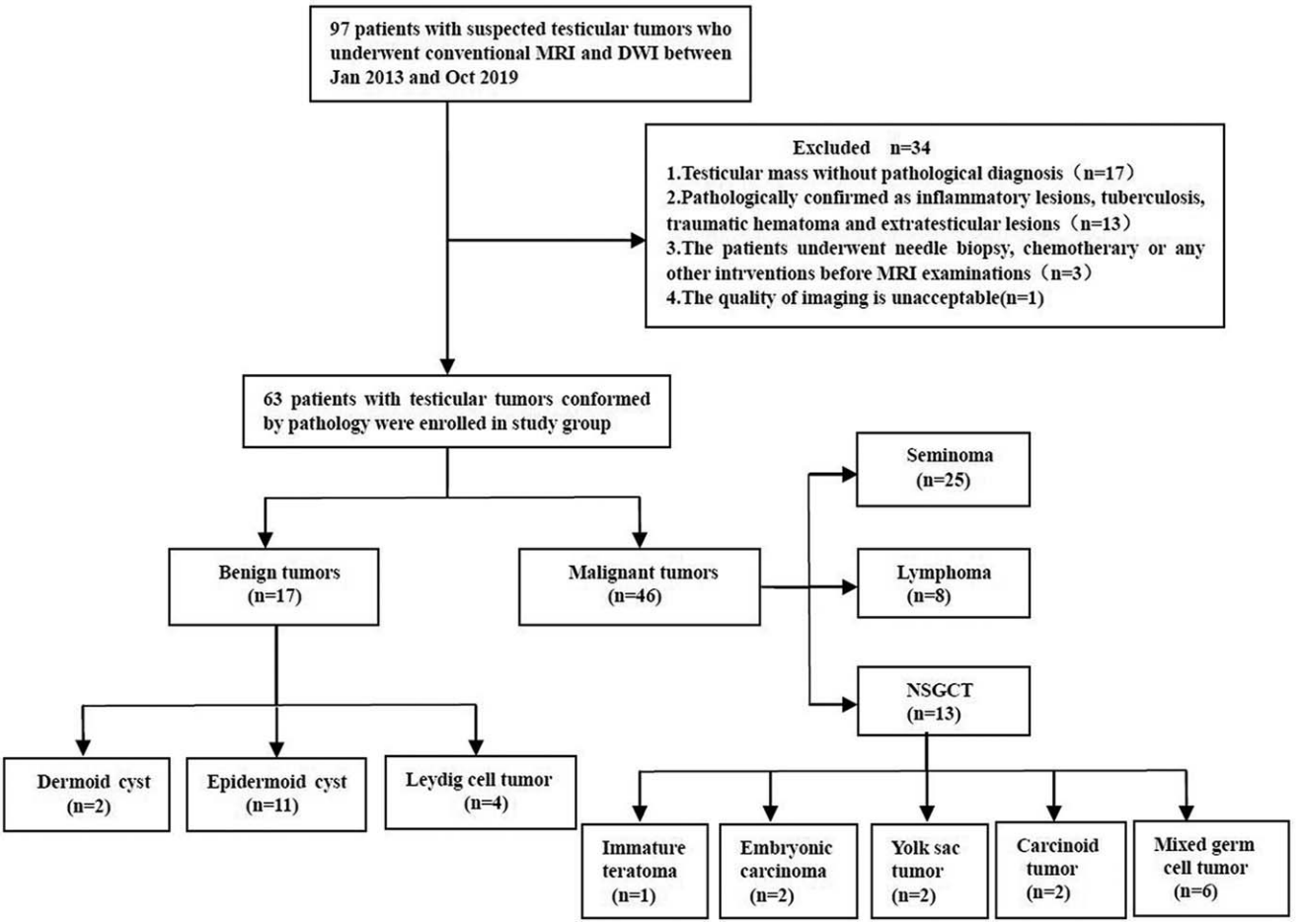

Figure 1. Flow chart depicting the patient screening process with exclusion criteria.

T2-weighted images not enhanced after gadolinium administration, representing cyst or necrosis); intratumoral septa (band-like structures of low signal intensity on T2-weighted images enhanced after gadolinium administration, recognized as fibrovascular septa.); capsule sign (T2-hypointense bands around the mass). According to the recommendations of the National Comprehensive Cancer Network and the European Germ Cell Cancer Consensus Group, the peritumoral infiltration of testicular tumors was graded into 4 categories. These 4 categories are as follows: T1 – tumor confined to the testis or extending through the tunica albuginea but not involving the tunica vaginalis; T2 – tumor involving the tunica vaginalis; T3 – tumor involving the spermatic cord; T4 – tumor involving the scrotal wall.[11]

The DWI data were transferred to the Siemens postprocessing workstation (syngo. via), and postprocessed with the mono-exponential model depicted in Eq. 1 where S(b) was the signal intensity at a b-value of 1000 s/mm^2, and S_{50} was the signal intensity at a b-value of 50 s/mm^2.

$$\frac{S(b)}{S_{50}} = e^{-(b-50)*ADC} \quad (1)$$

The ADC maps were automatically generated from DWI data. Taking the hyperintense signal area of the T2-weighted image and DWI as reference, regions of interests (ROIs) were drawn on images with b-values of 1000 s/mm^2 or 50 s/mm^2 (depending on which images displayed the lesion more clearly). The size of the ROIs was variable as they were drawn as large as possible and depended on the lesion size in a homogeneous low ADC region (avoiding hemorrhage and cystic areas). The ROIs were then automatically copied to ADC images.

2.4. Statistical analysis

The SPSS software version 17.0 (IBM Corp., SPSS, Chicago, IL) and Medcalc Version 12.7 (MedCalc, MedCalc Software, Mariakerke, Belgium) were used for statistical analysis, with $P < .05$ indicating statistical significance. Intraclass correlation coefficient (ICC) and kappa (weighted kappa if applicable) values were used to assess the reader agreements for continuous and categorical variables, respectively. Agreement was considered poor with ICC/kappa < 0.4; fair, 0.4 to 0.59; good, 0.6 to 0.74; and excellent, 0.75 to 1. The conventional MRI features were compared by using $\chi 2$ testing (the Fisher exact testing where appropriate) for categorical variables and a Kruskal–Wallis rank sum test for ranked data. The ADC values between all groups were compared using a Student *t* test and a one-way ANOVA. Then, significant conventional MRI features as well as the ADC values were included in multivariate logistic regression to create a conventional MRI model and a full model (conventional MRI model + ADC). Receiver operating characteristic (ROC) curve analysis was performed to determine the diagnostic accuracy and optimal cutoff ADC value in distinguishing malignant from benign masses. The area under the ROC curve (AUC) values, specificity and sensitivity were assessed as reported previously.[12] The DeLong method was used for pairwise comparisons between the AUCs of 3 models (ADC alone, conventional MRI alone, and full model). Multivariate logistic regression was also used to differentiate the histological subtypes of malignant tumors. The independent factors were obtained from all the parameters of conventional MRI and DWI.

3. Results

The interobserver consistency for routine MRI findings among the 63 cases was excellent as Kappa values ranged from 0.76 to 0.92 ($P < .05$). T2-homogeneity, intratumoral septa (Fig. 2) and peritumoral infiltration were more common in the malignant group, but capsule sign was more common in the benign group ($P < .05$). However, the differences of T2-homogeneity and cystic changes between the 2 groups were not statistically significant ($P = .800$, $P = .108$).

The inter-observer consistency for ADC values was excellent with an ICC value of 0.945 ($P < .05$). The mean ADC value of the malignant group was lower than that of the benign group ($P < .05$). The differences of conventional MRI features and the ADC value between benign and malignant intratesticular lesions are summarized in Table 1.

According to the conventional MRI model, T2-homogeneity, intratumoral septa, and peritumoral infiltration were significant independent factors for differentiating malignant testicular lesions from benign ones ($P < .05$). Moreover, the ADC value and T2-homogeneity, intratumoral septa, peritumoral infiltration were significant independent factors in the full model. The detailed description of these analyses is summarized in Table 2.

We also performed a ROC curve analysis using the ADC value, the conventional MRI model and the full model (Fig. 3). When the ADC value $\leq 0.90 \times 10^{-3}$ mm^2/s, the diagnosis tended to be a malignant lesion and the AUC was 0.739, the sensitivity was 70.6%, the specificity was 71.7%, and the accuracy was 71.4%. The conventional MRI model, including T2-hypointensity, intratumoral septa and peritumoral infiltration, achieved better diagnostic efficacy than the ADC value ($Z = 2.174$, $P = .030$). The full model (ADC + conventional MRI model) achieved better diagnostic efficacy than the ADC value ($Z = 2.938$, $P = .003$). The AUC of full model was not significantly different from that of the conventional MRI model ($Z = 1.496$, $P = .134$), but the specificity and accuracy increased by 9.8% and 3.2%, respectively. The AUC of the 3 models for the prediction of benign and malignant testicular tumors are shown in Table 3.

T2-homogeneity and T2-hypointensity (Fig. 4) were more common in seminoma and lymphoma ($P < .05$). Cystic changes (Fig. 5) were more common in nonseminomatous germ cell tumor (NSGCT) ($P < .05$). Intratumoral septa was more common in seminoma ($P < .05$). The ADC value of NSGCT was larger than seminoma, and lymphoma was the smallest, the differences between the 3 groups were statistically significant ($P < .01$). However, the differences of tumor staging among patients with lymphoma, seminoma, and NSGCT were not significant ($P = .159$). The details of the imaging characteristics and ADC values are summarized in Table 4.

Multivariate logistic regression analysis indicated that the ADC value and cystic changes were significant independent factors for differentiating NSGCT from seminoma [OR > 1000, 95% CI (3.52 ~>1000), $P = .024$; OR > 1000, 95% CI (1.844 ~>1000), $P = .033$]. The ADC value, cystic changes and T2-hypointensity were independent factors for differentiating NSGCT from lymphoma [OR > 1000, 95% CI (5.64 ~> 1000), $P = .004$; OR >1000, 95% CI (4.056 ~>1000), $P = .020$; OR > 1000, 95% CI (1.379 ~>1000), $P = .044$]. The ADC value and intratumoral septa were independent factors for differentiating lymphoma from seminoma [OR > 1000, 95% CI (29.281 ~>1000), $P = .023$; OR > 1000, 95% CI (1.705 ~>1000), $P = .042$].

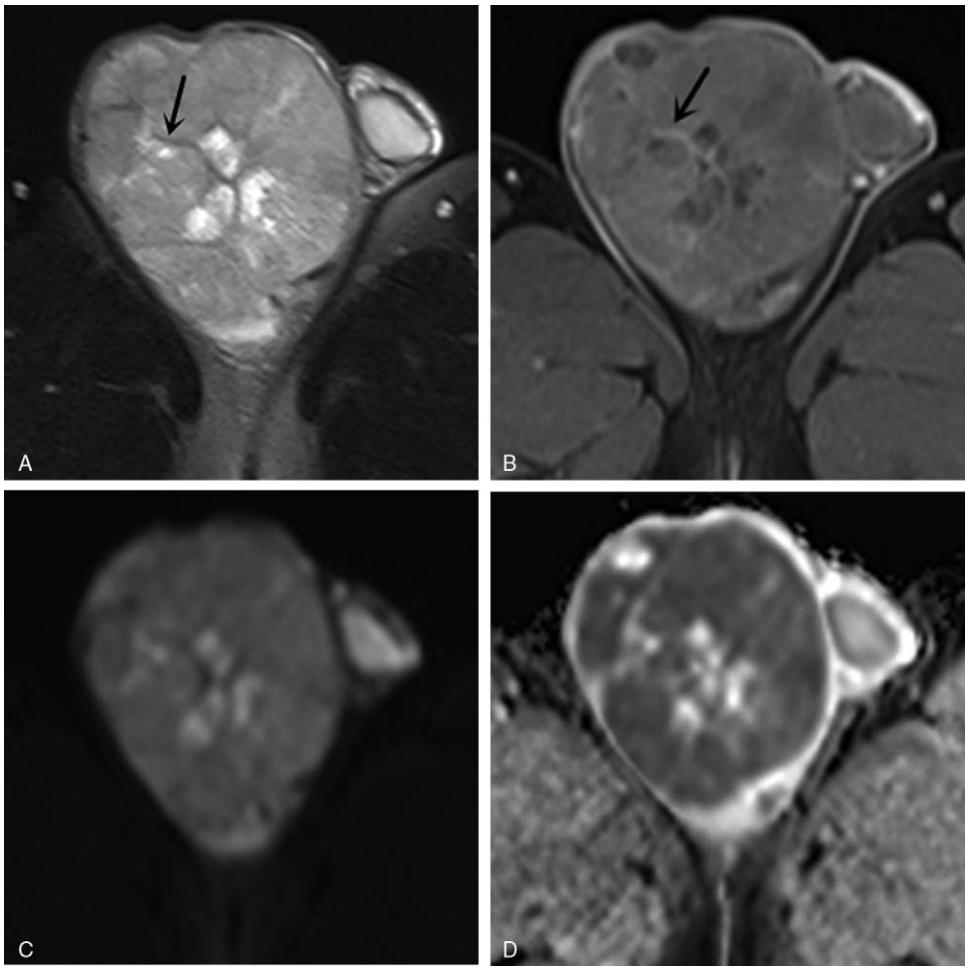

Figure 2. Images of a 47-year-old man with seminoma in right testis. (A) Axial fat-suppressed T2-weighted image shows a hypointense multinodular tumor with focal necrosis and hypointense septa (arrow). (B) Axial arterial phase fat-saturated gadolinium-enhanced T1-weighted image displays that the fibrous septa is more enhanced than the remaining tumor tissue (arrow). (C) Axial diffusion-weighted imaging (DWI) reveals a hyperintense mass with a mean apparent diffusion coefficient (ADC) value of $0.71 \times 10^{-3}\,mm^2/s$ (D).

Table 1

The conventional MRI findings and ADC values for benign and malignant intratesticular tumors.

Parameter	Malignant (n = 46)	Benign (n = 17)	t/χ^2	*P*
T2-homogeneity	20	8	0.064	.800
T2-hypointensity	23	3	5.360	.021
Intratumoral septa	28	5	4.925	.026
Cystic changes	22	12	2.589	.108
Capsule sign	11	12	12.478	<.001
Peritumoral infiltration	32	1	20.182	<.001
Albuginea/epididymis	20	1		
Tunica vaginalis	4	0		
Spermatic cord	7	0		
Scrotum	1	0		
ADC ($\times 10^{-3}$ mm^2/s)	0.79 ± 0.31	1.02 ± 0.40	−2.769	.007
≤0.90	34	6		
>0.90	12	11		

ADC = apparent diffusion coefficient.

Table 2

Multivariate logistic regression for differentiating benign and malignant intratesticular lesions.

	Conventional MRI model			Full model (ADC + conventional MRI model)		
Parameter	B	OR (95%CI)	*P*	B	OR (95%CI)	*P*
ADC				4.412	82.448 (1.628,4176.462)	.028
T2-hypointensity	2.515	12.363 (1.726,88.554)	.018	−3.105	0.045 (0.003,0.588)	.018
Intratumoral septa	2.356	10.547 (1.385,80.293)	.017	−2.993	0.050 (0.004,0.581)	.017
Peritumoral infiltration	−4.106	47.587 (3.547,638.424)	.005	−4.106	0.016 (0.001,0.288)	.005
Capsule sign	−0.424	0.655 (0.075,5.705)	.701	−0.424	0.655 (0.075,5.705)	.701
Constant term	−6.856	0.001	.002	−1.493	0.225	.426

ADC = apparent diffusion coefficient.

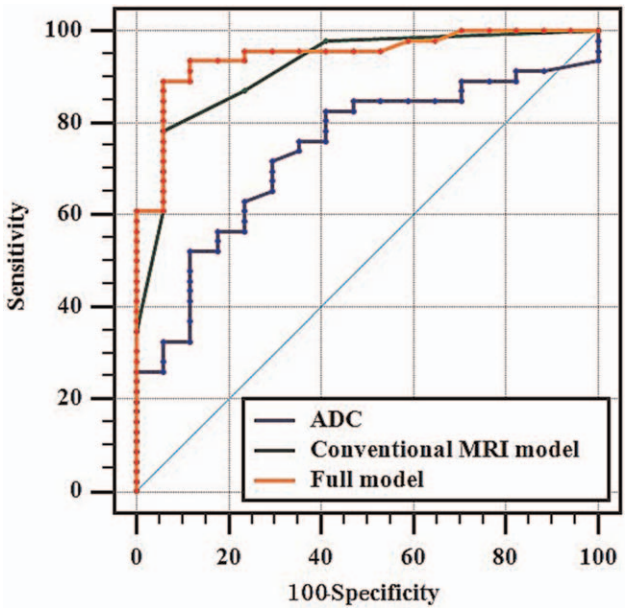

Figure 3. ROC curves of the ADC value model, conventional MRI model, and ADC value combined with conventional MRI model (full model) were used to distinguish benign and malignant testicular tumors. The AUCs of ADC (black line), conventional MRI model (green line) and full model (red line) were 0.739, 0.919, and 0.946, respectively. ADC = apparent diffusion coefficient.

4. Discussion

The primary conclusion of the present study is that ADC values are helpful in differentiating benign and malignant testicular lesions. Conventional MRI features are more powerful for such differential diagnosis; however, the combined ADC and conventional MRI model achieved better differential diagnostic efficiency than any individual parameter.

Due to the complex pathological components, the MRI findings of testicular tumors are relatively diverse. Tsili et al[13] revealed that some characteristic conventional MRI features, including the presence of heterogeneous T2-hypointensity, cystic changes and intratumoral septa and peritumoral infiltration, suggest malignancy. On the other hand, benign tumors usually display homogeneous signals, well-defined margins and an absence of contrast enhancement or slight enhancement on contrast-enhanced MR imaging. Consistent with previous reports, we found that T2-hypointensity, intratumoral septa and peritumoral infiltration were independent predictors of malignant testicular tumors.

The complex cell arrangement of testicular tumors limits the free diffusion of water molecules. Therefore, DWI exhibits hyperintense signals, while ADC shows hypointense signals.[14] We demonstrated that the ADC value of malignant testicular tumors is significantly lower than benign lesions. The ADC value of 0.90×10^{-3}mm^2/s is the diagnostic threshold for malignancy. Contrary to this result, Algebally et al[15] found that an ADC value of 0.99×10^{-3}mm^2/s was the diagnostic threshold for malignancy. The main reason for this difference may be that, in their study, the number of cases was small and the inclusion criteria was different for that in the current work. The previous study enrolled inflammatory and hemorrhagic lesion patients into the benign group. However, in our study, all 17 cases of benign lesions were neoplastic. Inflammatory lesions require anti-inflammatory treatment, while benign tumors can be treated with follow-up or conservative resection to preserve testicular function. Therefore, we do not recommend classifying these diseases into the same category. In addition, different MR scanners, parameters and ROI selections may have also led to different ADC diagnostic thresholds. Tsili et al[16] reported the combined usage of DWI and conventional MRI features for the

Table 3

AUC analysis of ADC and conventional MRI parameters for the prediction of benign and malignant intratesticular lesions.

Parameter	AUC	95%CI	Youden index	Sensitivity (%)	Specificity (%)	Accuracy (%)
ADC	0.739	0.609~0.904	0.423	70.6	71.7	71.4
Conventional MRI model	0.919	0.844~0.993	0.935	94.1	79.3	87.3
Full model	0.946	0.883~1.000	0.935	94.1	89.1	90.5

ADC = apparent diffusion coefficient.
Conventional MRI model: T2-hypointensity + Intratumoral septa + Peritumoral infiltration.
Full model: ADC+ conventional MRI model.

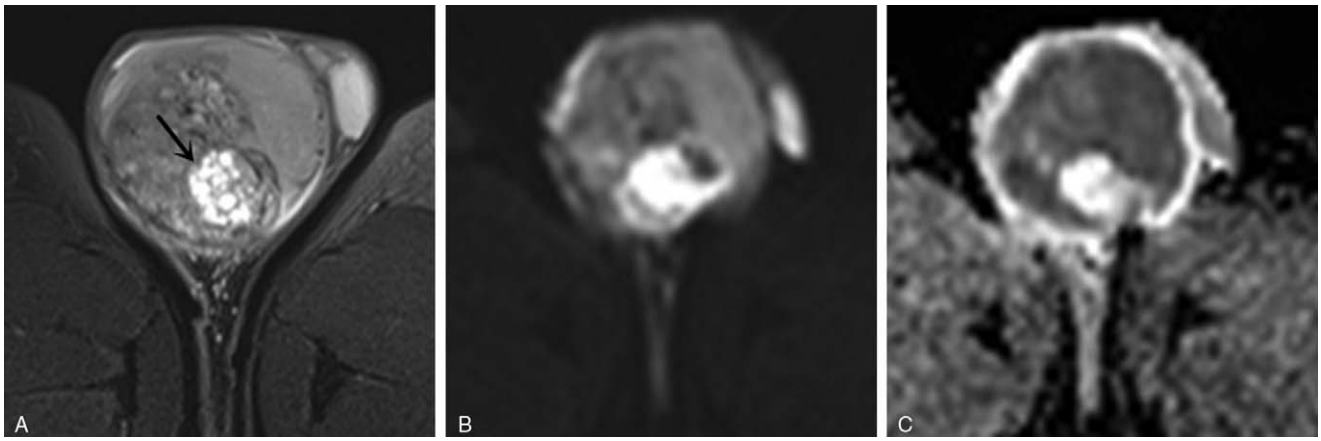

Figure 4. Images of a 41-year-old man with NSGCT in right testis. (A) Axial fat-suppressed T2-weighted image shows a hyperintense multinodular tumor with focal necrosis (arrow). (B) Axial DWI presents with heterogenous hyperintense signal with a mean ADC value of $0.83 \times 10^{-3}\,mm^2/s$ (C). ADC = apparent diffusion coefficient.

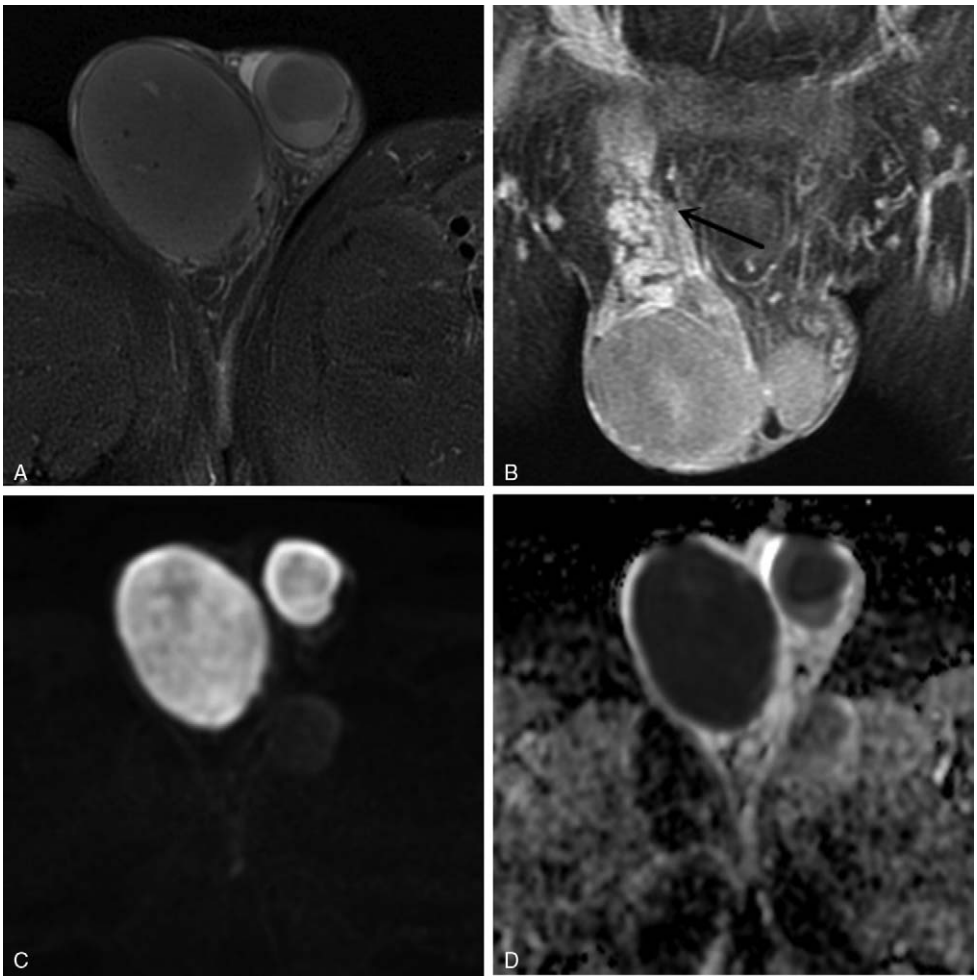

Figure 5. Images of a 63-year-old man with lymphoma in the bilateral testises. (A) Axial fat-suppressed T2-weighted image shows bilateral round-like tumors with hypointense signal. (B) Axial arterial phase fat-saturated gadolinium-enhanced T1-weighted image displays bilateral tumors with homogeneous enhancement and invasion of the right spermatic cord (arrow). (C) The bilateral masses present with heterogenous hyperintense signal on the DWI and heterogenous hypointense signal on the ADC image (D) with a mean value of $0.35 \times 10^{-3}\,mm^2/s$ (right), $0.48 \times 10^{-3}\,mm^2/s$ (left). ADC = apparent diffusion coefficient.

Table 4

The conventional MRI findings and ADC values for the testicular malignant tumor subgroups.

Parameter	Seminoma (n = 25)	NSGCT (n = 13)	Lymphoma (n = 8)	F/χ^2	P
T2-homogeneity	12	2	6	7.618	.022*,‡
T2-hypointensity	15	3	6	6.695	.035*,‡
Intratumoral septa	21	6	1	14.656	.001*,†
Cystic changes	11	13	1	17.646	.001*,‡
Capsule sign	7	3	1	0.807	.668
Peritumoral infiltration	15	9	8	4.581	.101
Albuginea/epididymis	11	5	4		
Tunica vaginalis	1	2	1		
Spermatic cord	3	1	3		
Scrotum	0	1	0		
Stage				3.681	.159
T1	21	9	4		
T2	1	2	1		
T3	3	1	3		
T4	0	1	0		
ADC values ($\times 10^{-3}$ mm^2/s)	0.75 ± 0.26	1.03 ± 0.31	0.50 ± 0.14	11.224	<.001*,†,‡

ADC = apparent diffusion coefficient, NSGCT = nonseminomatous germ cell tumor.

* $P < .05$, compared between seminoma and NGCT.

† $P < .05$, compared between seminoma and lymphoma.

‡ $P < .05$, compared between NSGCT and lymphoma.

differential diagnosis of testicular lesions, however, this work exhibited various limitations. Firstly, only 31 scrotal lesions were evaluated and ADC was not used as a quantitative indicator for analysis. Secondly, there was no comparative analysis on the diagnostic efficacy of DWI and conventional MRI. In the current study, we demonstrated the conventional MRI model achieved better diagnostic performance than the ADC model. Statistically better discriminative performance was further achieved after adding DWI to conventional MRI.

In previous studies, conventional MR features of different testicular malignancies were also variable. Seminoma and lymphoma present as hypointense signals in T2-weighted images because the tumor cells are densely packed with rare cystic changes.[17–20] NSGCT manifests as an inhomogenous hyperintense signal as it always contains more than 1 germ cell component or histologic subtype, the cystic changes are more common, and water content is higher than the normal testis.[21–23] Notably, hypointensity on T2-weighted image is not sufficiently specific to make an accurate diagnosis of seminoma. Rather, seminomas may be characterized by the presence of hypointense fibrovascular septa on T2-weighted image that are obviously enhanced.[24–26] In accordance with previous studies, we found that the T2-homogeneity and T2-hypointensity were more common in seminoma and lymphoma, and cystic changes were more common in NSGCT. Intratumoral septa was more common in seminoma than NSGCT and lymphoma.

The ADC values in the differentiation of seminoma and NSGCT had been documented in previous studies,[10,27] however, systematic discriminations for lymphoma with seminoma and NSGCT need further exploration. In the current study, the ADC value was an independent factor for quantitatively identify seminoma, NSGCT and lymphoma of the testis. We found that the mean ADC value of lymphoma was the smallest, followed by seminoma and NSGCT (largest). The pathological mechanism may be that lymphoma and seminoma have large, uniform cells with abundant cytoplasm and prominent nucleoli. These features likely contribute to reduce intra- and extra-cellular water motion, and reduced ADC values compared with NSGCT. Here, we demonstrated that ADC values combined with the most valuable conventional MRI features can differentiate lymphoma with seminoma and NSGCT, but the diagnosis performance needs further study.

We acknowledge limitations of our study. Firstly, the current work is a retrospective study with a relatively small cohort and potential selection bias needs to be considered. In addition, the different histologic subtypes of NSGCT were not separately analyzed due to the small number of cases. Secondly, exact ADC values were difficult to compare to other studies because of different coil systems, MR scanners, vendors, field strengths, b values and scanning parameters. Thirdly, conventional MRI features were assessed in a subjective manner and in the future more objective and quantitative measures should be utilized. Otherwise, in recent years, studies have shown that G-CSFR has the potential to promote tumor growth and metastasis.[28–31] Therefore, the clinical gene expression of G-CSFR in testicular tumors and its correlation with conventional MRI and functional MRI need to be further studied.

5. Conclusion

In conclusion, if testicular tumors are shown on MRI as a T2-hypointense signal, intratuminal septa, and peritumoral infiltration with an ADC value $\leq 0.90 \times 10^{-3}$mm^2/s, a malignancy diagnosis should be strongly considered. Therefore, ADC values combined with conventional MRI features may improve the diagnostic performance of testicular tumors. Moreover, combining MRI morphologic findings (cystic changes, T2-hypointensity, and intratumoral septa) with ADC values appears to be useful in differentiating seminoma, NSGCT, and lymphoma.

Acknowledgments

The authors thank Kai Meng and Huihui Zhou of Jining Medical University for guidance of statistical Analysis

Author contributions

Conceptualization: Weiwei Wang, Kewei Shi.
Data curation: Fan Zhao, Hao Yu, Xiang Guo.
Formal analysis: Weiwei Wang, Zhanguo Sun, Fan Zhao, Xiang Guo.
Investigation: Weiwei Wang, Hao Yu, Xiang Guo, Kewei Shi.
Project administration: Weiwei Wang, Zhanguo Sun, Yueqin Chen, Hao Yu.
Resources: Hao Yu.
Software: Fan Zhao, Hao Yu, Xiang Guo.
Supervision: Zhanguo Sun, Yueqin Chen.
Validation: Zhanguo Sun, Yueqin Chen.
Writing – original draft: Weiwei Wang.
Writing – review & editing: Kewei Shi.

References

[1] Albers P, Albrecht W, Algaba F, et al. EAU guidelines on testicular cancer: 2011 update. Eur Urol 2011;60:304–19.
[2] Oldenburg J, Fosså SD, Nuver J, et al. Testicular seminoma and non-seminoma: ESMO Clinical Practice Guidelines for diagnosis, treatment and follow-up. Ann Oncol 2013;24(Suppl 6):vi125–32.
[3] Vitolo U, Chiappella A, Ferreri AJ, et al. Firstline treatment for primary testicular diffuse large B-cell lymphoma with rituximab-CHOP, CNS prophylaxis, and contralateral testis irradiation: final results of an international phase II trial. J Clin Oncol 2011;29:2766.
[4] Gomez A, Santana PC, Mouro AP. Dosimetry study in head and neck of anthropomorphic phantoms in computed tomography scans. SciMed J 2020;2:38–43.
[5] Thomas LJ, Brooks MA, Stephenson AJ. The role of imaging in the diagnosis, staging, response to treatment, and surveillance of patients with germ cell tumors of the testis. Urol Clin North Am 2019;46:315–31.
[6] Qayyum A. Diffusion-weighted imaging in the abdomen and pelvis: concepts and applications. Radiographics 2009;29:1797–810.
[7] Saremi F, Knoll AN, Bendavid OJ, et al. Characterization of genitourinary lesions with diffusion-weighted imaging. Radiographics 2009;29:1295–317.
[8] Backens M. Basic principles and technique of diffusion-weighted imaging and diffusion tensor imaging. Radiology 2015;55:762–70.
[9] Yuan Y, Tang W, Jiang M, et al. Palatal lesions: discriminative value of conventional MRI and diffusion weighted imaging. Br J Radiol 2016; 89:20150911.
[10] Min X, Feng Z, Wang L, et al. Characterization of testicular germ cell tumors: whole-lesion histogram analysis of the apparent diffusion coefficient at 3T. Eur J Radiol 2018;98:25–31.
[11] Tsili AC, Argyropoulou MI, Giannakis D, et al. MRI in the characterization and local staging of testicular neoplasms. AJR Am J Roentgenol 2010;194:682–9.
[12] Song Y, Yoon YC, Chong Y, et al. Diagnostic performance of conventional MRI parameters and apparent diffusion coefficient values in differentiating between benign and malignant soft-tissue tumours. Clin Radiol 2017;72:e1–0.
[13] Tsili AC, Tsampoulas C, Giannakopoulos X, et al. MRI in the histologic characterization of testicular neoplasms. AJR Am J Roentgenol 2007;189:W331–7.
[14] Pedersen MR, Sloth Osther PJ, Nissen HD, et al. Elastography and diffusion-weighted MRI in patients with testicular microlithiasis, normal testicular tissue, and testicular cancer: an observational study. Acta Radiol 2019;60:535–41.
[15] Algebally AM, Tantawy HI, Yousef RR, et al. Advantage of adding diffusion weighted imaging to routine MRI examinations in the diagnostics of scrotal lesions. Pol J Radiol 2015;80:442–9.
[16] Tsili AC, Argyropoulou MI, Giannakis D, et al. Diffusion-weighted MR imaging of normal and abnormal scrotum: preliminary results. Asian J Androl 2012;14:649–54.
[17] Mittal PK, Abdalla AS, Chatterjee A, et al. Spectrum of extratesticular and testicular pathologic conditions at scrotal MR imaging. Radiographics 2018;38:806–30.
[18] Cassidy FH, Ishioka KM, McMahon CJ, et al. MR imaging of scrotal tumors and pseudotumors. Radiographics 2010;30:665–83.
[19] Mathur M, Mills I, Spektor M. Magnetic resonance imaging of the scrotum: pictorial review with ultrasound correlation. Abdom Radiol (NY) 2017;42:1929–55.
[20] Gupta R, Alobaidi M, Jafri SZ, et al. Correlation of US and MRI findings of intratesticular and paratesticular lesions: from infants to adults. Curr Probl Diagn Radiol 2005;34:35–45.
[21] Aganovic L, Cassidy F. Imaging of the scrotum. Radiol Clin North Am 2012;50:1145–65.
[22] Kim W, Rosen MA, Langer JE, et al. US MR imaging correlation in pathologic conditions of the scrotum. Radiographics 2007;27: 1239–53.
[23] Tsili AC, Sofikitis N, Stiliara E, et al. MRI of testicular malignancies. Abdom Radiol (NY) 2019;44:1070–82.
[24] Marko J, Wolfman DJ, Aubin AL, et al. Testicular seminoma and its mimics: from the radiologic pathology archives. Radiographics 2017;37:1085–98.
[25] Tsili AC, Giannakis D, Sylakos A, et al. MR imaging of scrotum. Magn Reson Imaging Clin N Am 2014;22:217–38.
[26] Liu R, Lei Z, Li A, et al. Differentiation of testicular seminoma and nonseminomatous germ cell tumor on magnetic resonance imaging. Medicine (Baltimore) 2019;98:e17937.
[27] Tsili AC, Sylakos A, Ntorkou A, et al. Apparent diffusion coefficient values and dynamic contrast enhancement patterns in differentiating seminomas from nonseminomatous testicular neoplasms. Eur J Radiol 2015;84:1219–26.
[28] Kosvyra A, Maramis C, Chouvarda I. Developing an integrated genomic profile for cancer patients with the Use of NGS data. Emerg Sci J 2019;3:157–67.
[29] Dwivedi P, Muench DE, Wagner M, et al. Time resolved quantitative phospho-tyrosine analysis reveals Bruton's tyrosine kinase mediated signaling downstream of the mutated granulocyte-colony stimulating factor receptors. Leukemia 2019;33:75–87.
[30] Dwivedi P, Muench DE, Wagner M, et al. Phospho serine and threonine analysis of normal and mutated granulocyte colony stimulating factor receptors. Sci Data 2019;6:21.
[31] Dwivedi P, Greis KD. Granulocyte colony-stimulating factor receptor signaling in severe congenital neutropenia, chronic neutrophilic leukemia, and related malignancies. Exp Hematol 2017;46:9–20.